Connection Design Recommendations for Improved BRBF Performance

KEITH D. PALMER, CHARLES W. ROEDER and DAWN E. LEHMAN

ABSTRACT

Numerous component tests on buckling-restrained braces (BRBs) have demonstrated their approximately symmetric tension and compressive capacities, stable cyclic behavior and large (component) ductility prior to core fracture. These properties make them suitable ductile fuses for seismic design. Experiments on buckling-restrained braced frame (BRBF) systems show that the inelastic axial deformation capacity of BRBs may be compromised by system performance demands. Damage including significant yielding, local buckling, twisting and fracture of the beams and columns, tearing of the gusset plate welds to framing members, and out-of-plane movement of the BRB have been observed in BRBF tests. Prior test results are reviewed, and an analytical study using high-resolution models, which were validated with prior test results, is used to develop mitigation strategies for the damage. Design recommendations to mitigate damage and improve system performance are developed. The study reveals that damage to the beams and columns at a corner gusset-plate connection is related to the ratio of the component web thickness to the gusset plate thickness, suggesting a modest design change that will significantly improve BRBF performance.

Keywords: buckling-restrained braced frames, ductile fuse, gusset-plate connection, core fracture.

INTRODUCTION

Buckling-restrained braced frames (BRBFs) are concentrically braced frames (CBFs) that utilize buckling-restrained braces (BRBs) to provide stiffness, strength and energy dissipation during an earthquake. Developed in Japan in the 1970s, BRBs are proprietary members that have become increasingly popular in the United States. As the name implies, a BRB prevents the brace from buckling in compression and, therefore, provides nearly symmetric force-displacement behavior in tension and compression. This results in superior energy dissipation capacity for the BRB component relative to a conventional buckling brace. A BRB consists of a steel core, which resists the axial load demands, and is placed inside a steel tube filled with a cementitious material to prevent buckling. Additional material is placed between the steel core and the cementitious fill to debond the steel core from the filled tube restrainer and limit transfer of axial load to the tube (Figure 1).

Keith D. Palmer, Structural Engineer, Simpson Gumpertz & Heger Inc., San Francisco, CA. E-mail: kdpalmer@sgh.com

Charles W. Roeder, Professor, Department of Civil and Environmental Engineering, University of Washington, Seattle, WA (corresponding). Email: croeder@u.washington.edu

Dawn E. Lehman, Associate Professor, Department of Civil and Environmental Engineering, University of Washington, Seattle, WA

Paper No. 2014-08R

The primary difference in design for different BRBFs lies in the connections as shown in Figure 2. Figure 2a shows a bolted connection of the cruciform shape of the BRB outside of the restraining tube for one BRB type. Figure 2b shows a clevis that is welded to an end plate, which in turn is welded to the BRB core and used to connect the BRB to the gusset plate. The pinholes in the gusset plate and clevis are reinforced to prevent a bearing failure, and this brace-to-gusset connection approaches a true pin about an axis perpendicular to the plane of the frame. In most cases, the beam is continuous between the faces of the two columns, but some BRBF connections have a beam moment release adjacent to the gusset as shown in Figure 2b to limit potential damage in the connection region. The connection of Figure 2c has a plate welded to the core end plate that is slotted to fit over the gusset plate and is welded to the gusset plate on four sides. Some connections have a collar that wraps around the BRB restrainer to add stability to the core extension beyond the filled steel casing, as shown in Figures 2b and 2c.

The design and testing of BRBs in the United States is governed by the AISC *Seismic Provisions* (AISC, 2010). These provisions focus on the tensile and compressive inelastic deformations of the BRBF under the design earthquake. The BRB must be designed, tested and detailed to accommodate expected deformations associated with a story drift of at least 2% of the story height or two times the design story drift, whichever is larger, in addition to the brace deformations associated with frame deflection due to gravity loading. BRBs must pass qualifying cyclic brace component and subassemblage tests as specified in Section K3 of the *Seismic Provisions*. The component test consists of cyclic uniaxial loading, but the subassemblage test also simulates connection rotational demands on the BRB caused by frame action. The BRB must achieve a cumulative inelastic deformation capacity of 200 times the yield deformation or greater in the component test.

Recent experiments on BRBF systems suggest that the BRB may reach its expected strength and deformation capacity, but the *system* deformation capacity may be limited by damage to other components or by unintended system response mechanisms (Palmer et al., 2014). As a consequence, the BRBF system performance is often more complex than suggested by current design methods.

SUMMARY OF PRIOR RESEARCH RESULTS

Experimental Research

Numerous component tests (e.g., Black et al., 2004; Merritt et al., 2003; Romero et al., 2007) have been performed on BRBs in the United States, and these tests demonstrate the ability of the BRB component to achieve ductility and cumulative inelastic deformation greater than demands expected during the design basis and the maximum considered earthquakes.

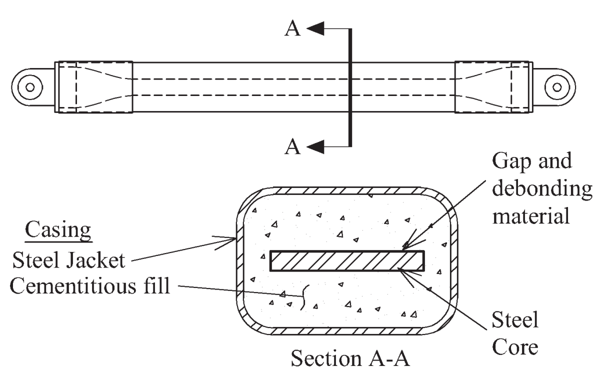

Fig. 1. Typical design of BRB.

Uriz (2005) tested three large-scale, partial, two-story, one-bay, planar BRBFs, and Christopolus (2005) tested five full-scale, single-story, one-bay, planar BRBFs. The BRB ductility values achieved during these tests ranged between 14 and 22, which are comparable to those achieved in BRB component tests. Additionally, the cumulative ductility values achieved in these BRBF experiments exceeded the minimum value of 200 required by the *Seismic Provisions* for BRB component tests. However, significant column and/or beam yielding and local buckling and tearing of flanges, welds and gusset plates occurred in these tests such as illustrated in Figure 3a. In many cases, out-of-plane rotation of and plastic hinge formation in the BRB core plate outside of the restrainer occurred at story drift ratios less than 2.5% as illustrated in Figure 3b. This plastic hinge formation was likely a consequence of a combination of frame yielding and deformation and the stiffness of the gusset plate and unrestrained BRB core.

Fahnestock et al., (2007) tested a 0.6-scale, four-story, planar, one-bay BRBF, in which the frame beam fixity was released at the gusset plate connections through a web-only connection similar to that shown in Figure 2b. The maximum ductility achieved by the BRBs ranged between 18 and 26, and the cumulative ductility ranged between 388 and 453, which are much larger than the 200 required by the *Seismic Provisions*. No undesirable behaviors were observed during the experiment prior to BRB fracture, and this may be at least partially attributed to the beam-moment release connection detail (see Figure 2b).

A large-scale, two-story, one-bay by one-bay, three-dimensional BRBF was tested (Palmer, 2012). The BRBs were placed in two orthogonal bays, with a single BRB in

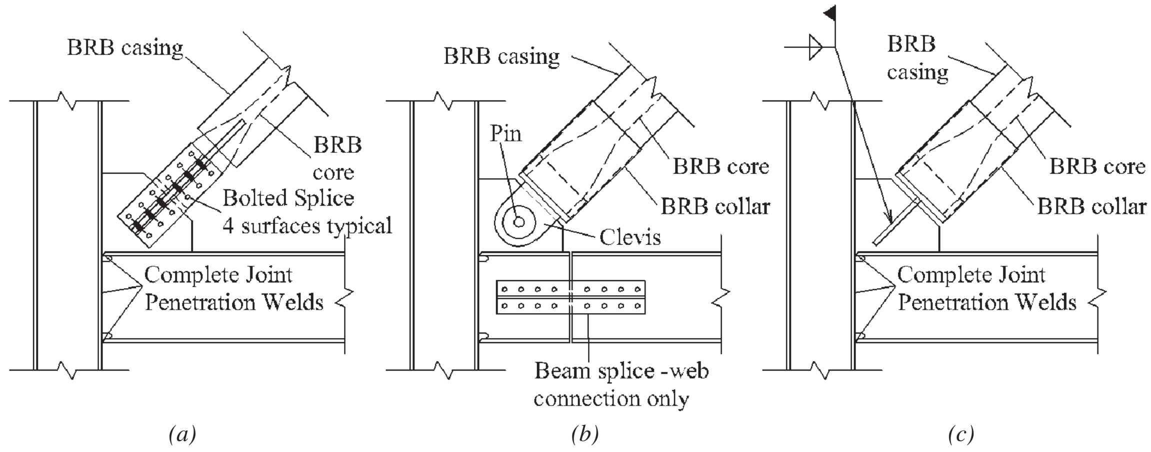

Fig. 2. BRB connection types: (a) bolted BRB, fixed beam; (b) pinned BRB, pinned beam; (c) welded BRB, fixed beam.

each story (Figure 4a); the remaining bays were designed and detailed as gravity frames. The floor system consisted of intermediate beams and composite slab on metal deck on the first level, to simulate the strength and stiffness of the floor system, and a reinforced concrete slab on the second level, to also transfer loads to the frame from the actuators. A bi-directional, cyclically increasing displacement history was applied to the top floor of the system. In the braced bays, the beam flanges and webs were attached to the columns with complete-joint-penetration (CJP) welds. The gusset plates were attached to the beams and columns with fillet welds sized according to the uniform force method (with interface moments included) and the *Seismic Provisions* (AISC, 2005, 2010) using overstrength factors corresponding to 3% story drift. The welds were performed by AISC-certified welders and visually inspected afterward. The beams and columns were checked to ensure that they passed the web crippling and web yielding checks. The dimensions and member sizes of the south frame (frame 1) are shown in Figure 4b. Additional information may be found elsewhere (Palmer, 2012).

Significant BRBF damage concentrated adjacent to the beam-column-gusset plate connections was observed (Palmer et al., 2014), and very little damage was observed at joints without gusset plates. Tearing of the gusset plate–column interface welds occurred when the brace was in compression, and these tears propagated the total length of the weld in three locations by story drifts ranging between 2.3 and 2.9%, as illustrated in Figure 3c. The BRBs were still performing well after these tears, and no other negative behaviors were observed due to these tears. Local flange and web buckling occurred at the base of two braced frame columns and in the beams adjacent to the gusset plate corner connections at approximately 2.5% story drift. Extensive beam flange and web tearing and fracture occurred at approximately 3.5% story drift. Column flange and web tearing also occurred in one location (second floor in the right

(a) (b) (c) (d)

Fig. 3. Damage noted in prior BRBF test results: (a) yielding of beams and columns; (b) out-of-plane movement of BRB; (c) gusset weld fracture; (d) fracture through column flange and web.

column in Figure 4b) and initiated in the column k-region at the CJP weld connecting the braced frame beam bottom flange to the column as shown in Figure 3d. The bolts in the column web are for the transverse gravity beam connection. The second-story BRBs fractured at 4.2 and 3.6% story drift in frames 1 (in foreground) and B (on right), respectively.

Analytical Research

Accurate simulation of BRBFs cannot be accomplished with simple line-element modeling because these models do not capture the complex nonlinear interaction among BRBs, other framing members and their connections. Most researchers have used continuum models, which simulate nonlinear performance but have limitations in modeling tearing and fracture of welds or steel. Fracture due to ultra-low-cycle fatigue occurs after a relatively small number of cycles at large inelastic strains, and therefore, both cyclic and maximum strain indices have been considered by researchers to implicitly predict fracture or tearing (Palmer, 2012).

Wigle and Fahnestock (2010) used ABAQUS to simulate the BRBF tested by Fahnestock et al., (2007). The third story of the test frame, including the BRB, was modeled with shell elements. The BRB casing was modeled using a flexurally stiff and axially flexible line element for the casing element that was connected to the nodes of the BRB core shell element. This approach prevented buckling of the core and minimized the axial load in the restrainer. The beams and columns in the lower two stories of the frame were modeled using line beam-column elements with lumped plastic hinges at the ends, and the BRBs were modeled as nonlinear axial springs. The simulated BRB response matched the global experimental response for the drift ranges simulated. The model was used to study the effect of bolted, pinned and welded BRB end connections; fully restrained and moment release beam end conditions; and gusset plate thicknesses [0.25 and 1.0 in. (6.35 and 25.4 mm)]. The results indicated that the type of BRB-to-gusset plate connection did not significantly affect the force-deformation behavior or local strain demands in the gusset plate connection region. Thicker gusset plates induced larger plastic strain demands at the interface of the gusset plate with the beams and columns but did not affect the global response.

This brief summary of prior research shows that the excellent component behavior measured for BRBs does not necessarily translate to equivalent system behavior. BRBF system performance often fell short of the expected performance based on the component results. Experiments on BRBF systems can be used to evaluate mechanisms to improve the system response, but experiments are too costly for evaluation of all critical parameters. Therefore, this paper describes the use of robust, high-resolution numerical simulation for this purpose.

FE MODELING APPROACH

The ABAQUS analysis platform (ABAQUS, 2010) was used to accurately simulate the global and local responses of the BRBF test specimen shown in Figure 4 and summarized

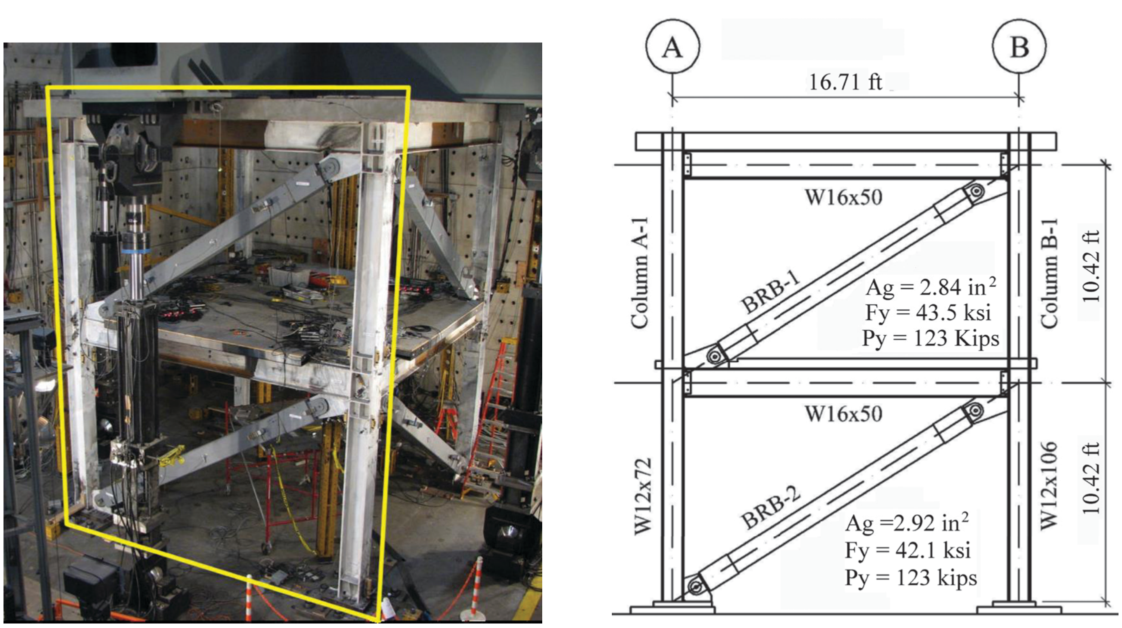

(a) (b)

Fig. 4. BRBF used for finite element simulations: (a) experimental frame; (b) frame elevation (Palmer, 2012).

earlier (Palmer, 2012). Variations on that basic model were then made to study selected parameters. The test specimen had two orthogonal and adjacent braced bays, but the ABAQUS model simulated only one planar braced frame as highlighted in the foreground in Figure 4a and shown schematically in Figure 4b.

Beams, columns, slabs and connections were modeled using three- and four-node quadrilateral shell elements as shown in Figure 5. The shell elements had six degrees of freedom per node. First-order (linear-interpolation) elements with reduced integration and hourglass control were used to reduce runtime and prevent locking and zero-energy deformation modes. Transverse shear stiffness was included in the formulation of the shell sections, which had five layers through the thickness and were numerically integrated during the analysis to calculate cross-sectional behavior.

The BRBs were modeled using nonlinear truss elements because of the complications and computational expense involved in modeling the core, end collars, steel tube restrainer, infill grout, contact and friction between these elements, and higher-mode core buckling. Greater modeling accuracy, using shell elements for the BRB and a line-element casing model following Wigle and Fahnestock (2010), was deemed unnecessary in this study as BRB performance was secondary to frame behavior caused by BRB forces. The truss element was calibrated to measured BRB behavior and provides accurate simulation of the local and global performance of the BRBF system.

The base of each column was fully restrained in the three orthogonal directions as shown in Figure 5. Out-of-plane restraint was provided to the braced frame beams at mid-span where transverse floor beams framed into them in the

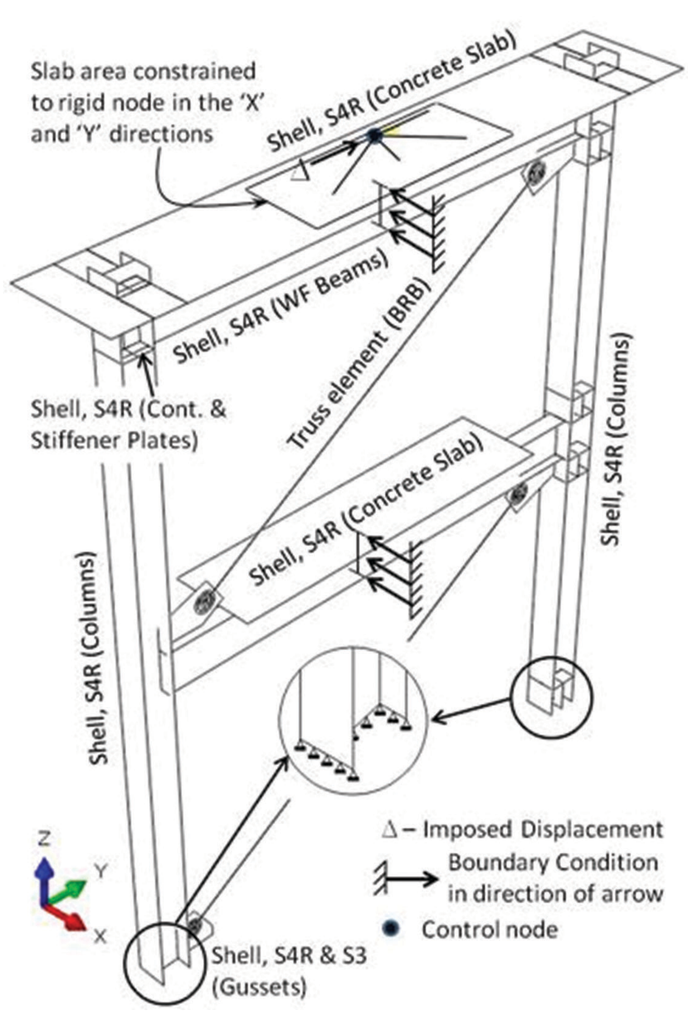

Fig. 5. BRBF finite element model with element types and boundary conditions (see Figure 3b for component sizes and frame dimensions).

Table 1. Material Yield Strengths from 3D BRBF Experiment (Palmer, 2012)		
	Measured Properties	
Shape	F_y ksi (MPa)	F_u ksi (MPa)
W12×106	55.5 (386)	73.4 (510)
W12×72	56.5 (393)	72.4 (503)
W12×45	56.5 (393)	71.4 (496)
W16×50	52.5 (365)	68.5 (476)
W16×31	54.5 (379)	68.5 (476)
W14×22	54.5 (379)	67.5 (469)
BRB-1 core	43.0 (299)	62.7 (436)
BRB-2 core	41.7 (290)	64.5 (448)

test frame. In the laboratory, the displacement history was applied to the test specimen through a large, strong, and stiff crosshead attached to the floor slab. In the analysis, a rigid control node was used to apply the displacement history of the frame (shown at the top of the frame in Figure 5). The movement of the third floor slab was constrained to the movement of this control node. The concrete slabs were simulated with shell elements, which were linked to the shell elements of the steel beam to develop composite action. Kinematic coupling constraint tied the top floor slab degrees of freedom in the area outlined in the figure to the control node. The width of the concrete slab was defined by the effective width design rules of the *Seismic Provisions*. The cyclic displacement history for the test frame was bi-directional, and the specific deformations applied to the simulation at the control node of frame 1 are shown in Figure 6.

Geometric nonlinearities were included in the analyses using the updated Lagrangian approach to capture local (and global if it occurs) buckling of the beams, columns and gusset plates. In this approach, the element stiffness is formulated at each step using the nodal coordinates in the current, deformed configuration.

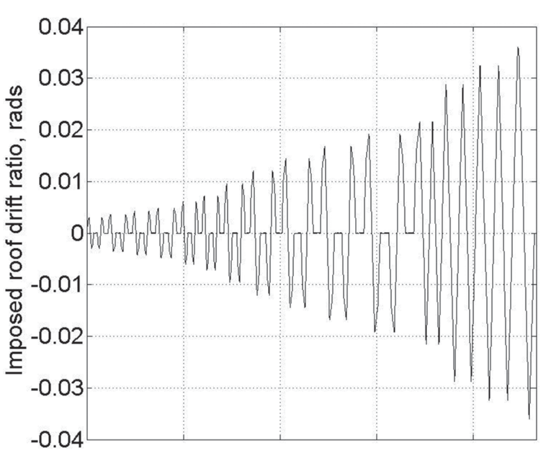

Fig. 6. Imposed cyclic displacement protocol in experiment (Palmer, 2012) and finite element simulation.

The concrete was modeled using a linear, elastic constitutive model because minimal cracking and crushing were observed during the testing. The steel yield strengths were obtained from mill test certificates and test coupons (see Table 1), while the concrete strength and elastic modulus was obtained from cylinder tests. Twenty-eight-day compressive 4 × 8 cylinder strengths of 6 and 8 ksi (42 and 55 Mpa) were measured for the second and third floor slabs, respectively. Steel material nonlinearities were simulated using the von Mises yield criterion with an associative flow rule and a combined, nonlinear kinematic and isotropic hardening law.

A mesh refinement study was performed to balance convergence and accuracy with minimizing the run time. Four models with different mesh densities were analyzed, and the average element sizes in the connection region ranged between 0.5 and 2.0 in. (12.7 and 50.8 mm). The results indicated that a mesh size of 1 in. (25.4 mm) was needed in the connection regions. A 2-in. (50.8-mm) mesh size was used in regions away from the connection regions (Palmer, 2012). The connection regions are defined as the area in the beams and columns that extend approximately three times the depth of the beam in each direction from the intersection of the column and beam centerlines.

Fracture is not simulated directly by the ABAQUS computer program. El-Tawil et al., (2000) and Kanvinde and Deierlein (2006) showed that tearing and fracture can be predicted using FEA and a micromechanics-based approach. That approach uses the strain at ductile fracture initiation according to Hancock and Mackenzie (1976), which is a function of a material constant and the stress triaxiality ratio. This strain is then divided by the cumulative equivalent plastic strain (PEEQ) multiplied by the material constant needed to define a rupture index. This rupture index is used as an indicator of the susceptibility of the material to fracture. Studies confirm the accuracy of this approach (e.g., Chao et al., 2006), but this method requires very small, eight-noded brick elements with dimensions on the order of the characteristic length of the material [0.1 in. (0.3 mm) for structural steel], which results in a large computational expense.

Yoo (2006) investigated and validated the use of strain indices in shell element models for predicting initial gusset plate weld tearing as part of a prior study on special concentrically braced frames (SCBFs). Two indices were investigated: the equivalent plastic strain (PE) and the PEEQ. The simulation results of concentrically braced frame (CBF) systems experiments indicated a strong correlation between the PE with the first instance of observed tearing in the hollow structural section (HSS) braces and gusset plate, and this approach was used in this study.

MODEL VALIDATION

The model was validated using three categories of metrics: (1) global response, (2) observed damage modes and (3) local deformation measures.

Global response depends on accurate simulation of the BRB. BRB response is not completely symmetric because the compression overstrength and isotropic hardening vary with axial strain and history. However, a truss element with the von Mises yield criterion provides symmetric behavior. As a result, the BRB truss element was calibrated to (1) reach the average of the maximum tension and compression strengths, (2) match the initial yield load, (3) match the total energy dissipated and (4) match the residual load at zero displacement.

The simulated and measured force-displacement responses of the second-story BRB at four different story drift levels are shown in Figure 7a. At small story drifts, the elastic and inelastic behavior is accurately captured. At large inelastic deformations, the simulated tensile resistance and hardening slope are larger than the measured slope, while the compressive resistance and hardening slope are underestimated. However, the ultimate objective of the analytical study was to provide relative comparisons between different connection designs. Relative differences among the models are independent of the BRB material model (Palmer, 2012); therefore, this approximate simulation of the strength was deemed appropriate.

Figure 7b shows the total base shear as a function of the average story drift of the top of the frame. There is excellent agreement between the measured experimental results and the simulation. Fracture was not simulated, and therefore, the loss in strength resulting from BRB fracture is not captured in the FE model.

Figures 7c and 7d compare the experimental and simulated third-floor beam deformation within the gusset plate connection region at approximately 3.5% story drift. The figures show excellent agreement of the local flange buckling and out-of-plane web deformation at this location. Similarly, excellent agreement is observed in the simulated and tested models at the base of column A-1, as shown in Figures 7e and 7f. This buckling mode occurred at the base and not at the elevated gusset plate. The difference in the buckling modes at these two locations results from the difference in the boundary conditions. These comparisons show that the ABAQUS model provides accurate local and global simulation of the true BRBF behavior.

PARAMETRIC STUDY OVERVIEW

After verification of the accuracy of the basic model, that model was expanded to investigate salient parameters that affect the BRBF response and to evaluate potential improvements to BRBF design. Approximately 50 different models were analyzed to study the effects of:

1. Gusset plate thickness.
2. Gusset plate taper.
3. Gusset plate edge reinforcement.
4. Beam reinforcement at the joint, including web doubler plates (see Fig. 8) and flange stiffeners.
5. Column size and reinforcement at the joint, including web doubler plates (see Fig. 8) and continuity plates.
6. Beam fixity at joint region.
7. Variations in modeling the interface weld connecting the gusset plate to the beams and columns.
8. Strength and stiffness of BRB.

The reference model for the parameter study was the three-dimensional test frame model described earlier. All other analyses had well-defined variations from the reference model to evaluate the parameter in question. Comparisons and evaluations were based upon three performance metrics.

1. *Global force-displacement and local moment-displacement relationships* were compared to establish relative stiffness, resistance and initiation of strength degradation for a given model. Early strength degradation clearly represents substandard performance.
2. *The computed von Mises stress distributions and deformed shapes* were compared in critical regions (including gusset plates, beams and columns adjacent to the gusset) to identify potential locations of concern (see Figures 7d and 7f for an example).

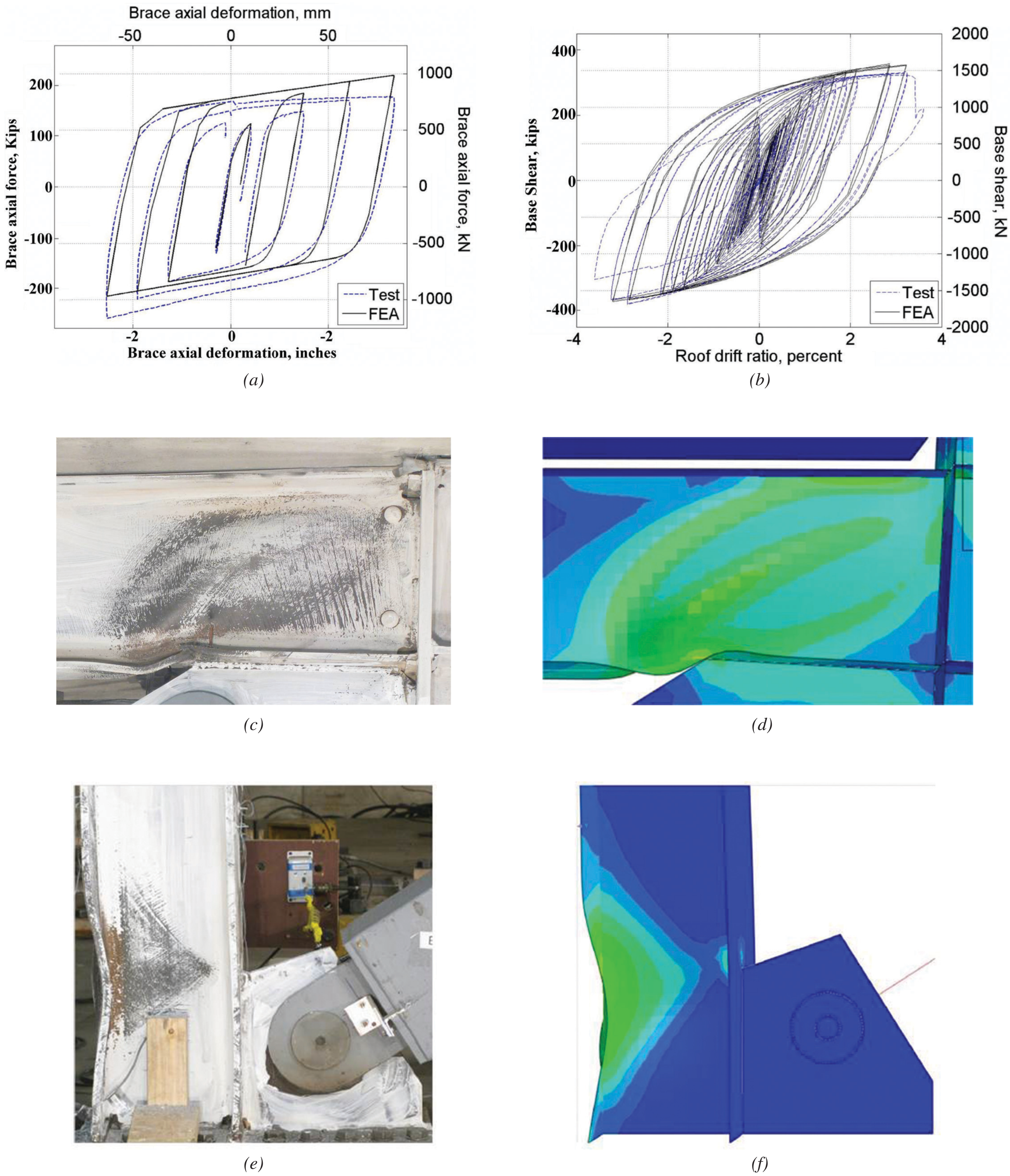

Fig. 7. Reference model validation: (a) BRB force-deformation response; (b) global base shear-story drift response; (c) observed beam yielding and local buckling; (d) simulated beam yielding and local buckling: (e) observed column yielding and local buckling; (f) simulated column yielding and local buckling.

3. *Local strains along the gusset plate interfaces with the beams and columns* were compared to identify weld yielding and potential crack initiation or fracture. The PE and PEEQ values were compared as approximate indicators of potential crack initiation and fracture (Yoo, 2009).

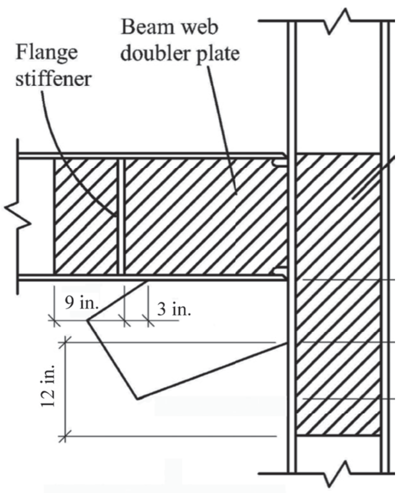

Fig. 8. Finite element model details: beam and column reinforcement.

These performance indices were evaluated at story drift levels of 2 and 3.5% because these drift levels approximate the design basis and the maximum considered earthquake demands, respectively (Chen et al., 2008). The stresses and strains sampled in the beams and columns at gusset plate interfaces were the average of the two elements simulating fillet welds on either side of the gusset plate. The gusset plate stresses and strains were sampled from single elements that occurred at the interface, as shown in Figure 9a. Typical plots of the PEEQ as a function of distance along the edge of the gusset from the intersection of the beam and column flanges (corner of the gusset) are illustrated in Figure 9b, and maximum PEEQ values in the beam, column and the edges of the gusset plate at 2% story drift are listed in Table 2. The table also lists the peak base shear and peak moment at the top of the right column in the second story. The maximum PEEQ invariably occurred at locations shown in Figure 9b.

ANALYSIS RESULTS

The initial stiffness values of all models were within 5% of each other; this is logical because the BRB provides the main contribution to elastic stiffness. The columns (W12×106 and W12×72) used in the test frame were larger than required by current seismic provisions (due to multiple tests performed on the frame), so smaller permissible columns (W12×50)

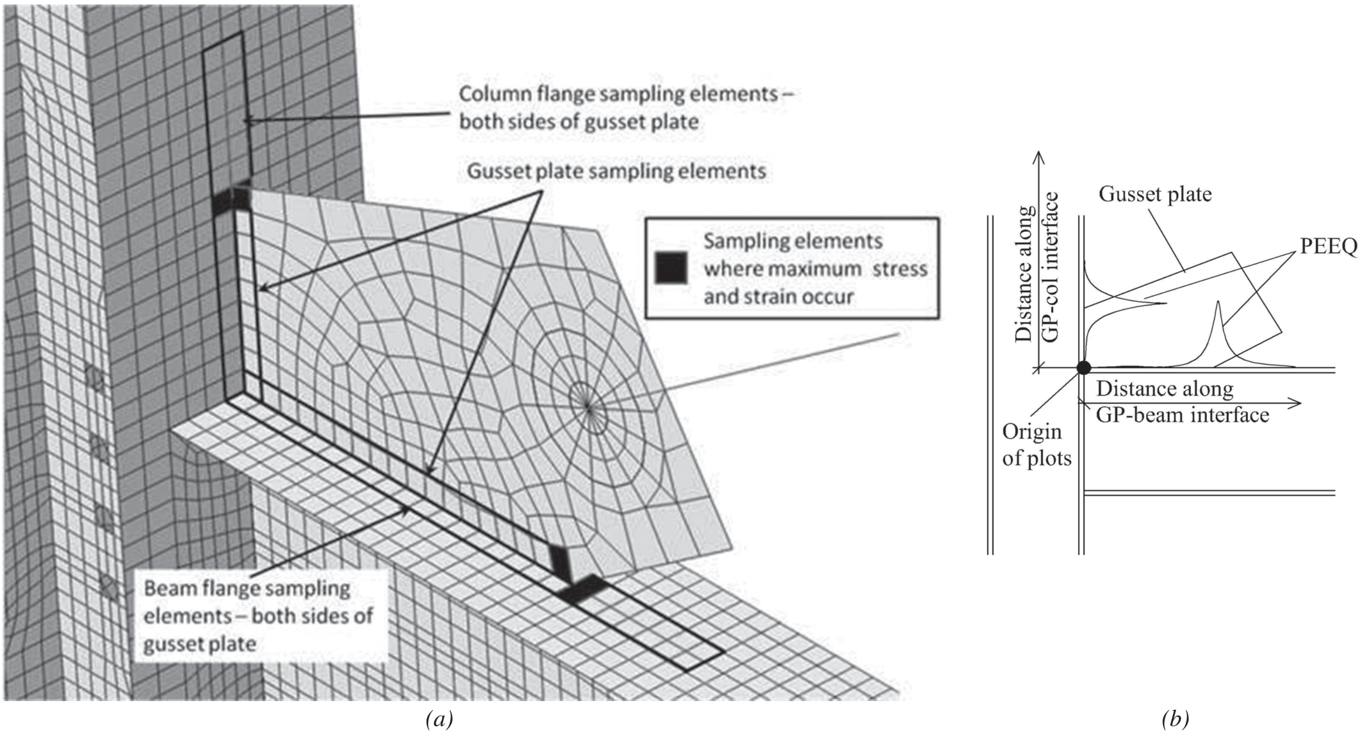

Fig. 9. Finite element simulation performance indicator sampling regions: (a) elements sampled within connection region; (b) schematic description of plots used in comparisons.

were investigated along with potential reinforcement to critical areas of the smaller columns. The peak base shears were similar for all models with the same columns, but models with the smaller columns developed a base shear force that was 9 to 15% less than the reference model. The smaller column resisted approximately half the shear of the larger column in the reference model.

Reinforcement of Beam and Column Webs

While some columns were larger than required in the three-dimensional test specimen, significant damage was noted in nearly all beams and columns adjacent to gusset plates in test frames. This raises logical questions as to how the specimen would have performed if the minimum permissible column were employed and how damage can be reduced in the beam and column locations without excessively increasing beam and column sizes. Figure 10 plots the envelope of the cyclic moment-story drift response, where the moment is measured at the top of the column of the second story for four different models. The analysis shows that the reference model (test specimen) provided somewhat larger base shear resistance than the model with weaker columns because of the larger column shear resistance provided as noted earlier. The figure also shows that deterioration in resistance occurred with both the reference model and the reduced column model due to the inelastic damage in the beam and column, which included local buckling, but the deterioration and damage were significantly greater with the smaller column. The figure shows that the addition of web reinforcement (a doubler plate to the column web to create a column web thickness of 75% of the gusset plate thickness) eliminated the deterioration of resistance and reduced column damage for both the reference column and the smaller column specimen. While the addition of column web reinforcement reduced damage to the column, it invariably increased damage to the beam unless comparable measures were taken for the beam web.

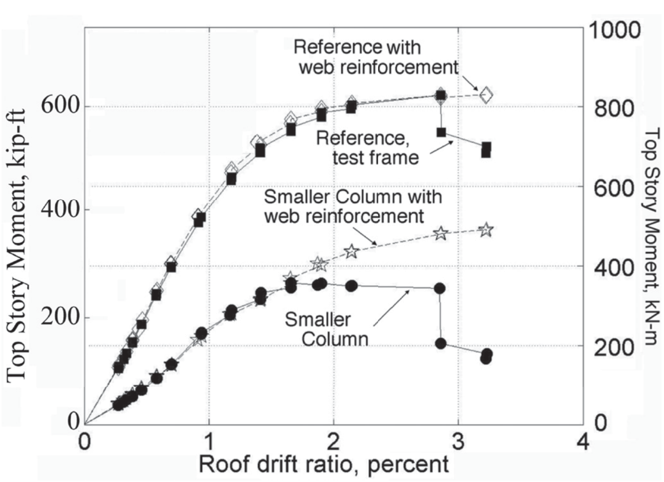

Fig. 10. Moment-story drift backbone at top of second-story column.

Comparison of analytical results in Figure 11 amplifies these observations and also shows the effect of local damage to the beam. Figure 11a shows the extensive damage to the beam and lesser damage to the column for the reference specimen at 3.5% story drift for one connection in the frame. It must be emphasized that the ABAQUS model does not directly include cracking, tearing or fracture, and prior discussion has demonstrated extensive cracking and fractures in beams, columns and gussets at deformations well below this level. Figure 11c shows the increased damage to the column web and reduced damage to the beam if the lighter column is employed. Figure 11b shows the reduced damage to the beam web if the web of the reference model is reinforced as noted earlier, while comparison of Figure 11c and 11d shows the reduced damage and stress levels in the column when the web of the smaller column is reinforced. Finally, Figure 11e shows that the reduced damage to both the beam and the column webs is reinforced with the model with the lighter column section. These comparisons show that the addition of web reinforcement to create a total effective thickness of 75% of the gusset plate thickness eliminated all damage to the beam and the columns and significantly changed and reduced local stress demands in the beam and column webs.

Extensive beam and column damage was observed in the experiment, and the comparisons in Figures 10 and 11 suggest that the relative thickness of the gusset plate to beam and column web thickness is a contributing cause of this damage. In the experiments, the relatively thicker gusset plates sustained minimal yielding in contrast to the extensive yielding in the relatively thin beam and column webs. In addition, the gusset plate welds sustained damage. This is logical when considering that the webs of the W16×50 beam, W12×72 column and W12×106 column were 0.38, 0.43 and 0.61 in. (9.7, 11 and 15.5 mm) thick, respectively, while the gusset plates were 1 in. (25.4 mm) thick. The stress in the gusset plate has a direct path into the beam and column web, so a BRB that requires a thick gusset plate should also require a relatively thick beam and column web. This situation is aggravated with BRBs as compared to buckling braced frames because brace buckling reduces stress demands on the gusset although increasing deformation demands on the gusset.

Analyses were performed to evaluate this observation. Stresses in the beam and column webs may be reduced by increasing the thickness of the beam and column web by the addition of web reinforcement, decreasing the thickness of the gusset plate, or changing the connection configuration to alleviate the problem.

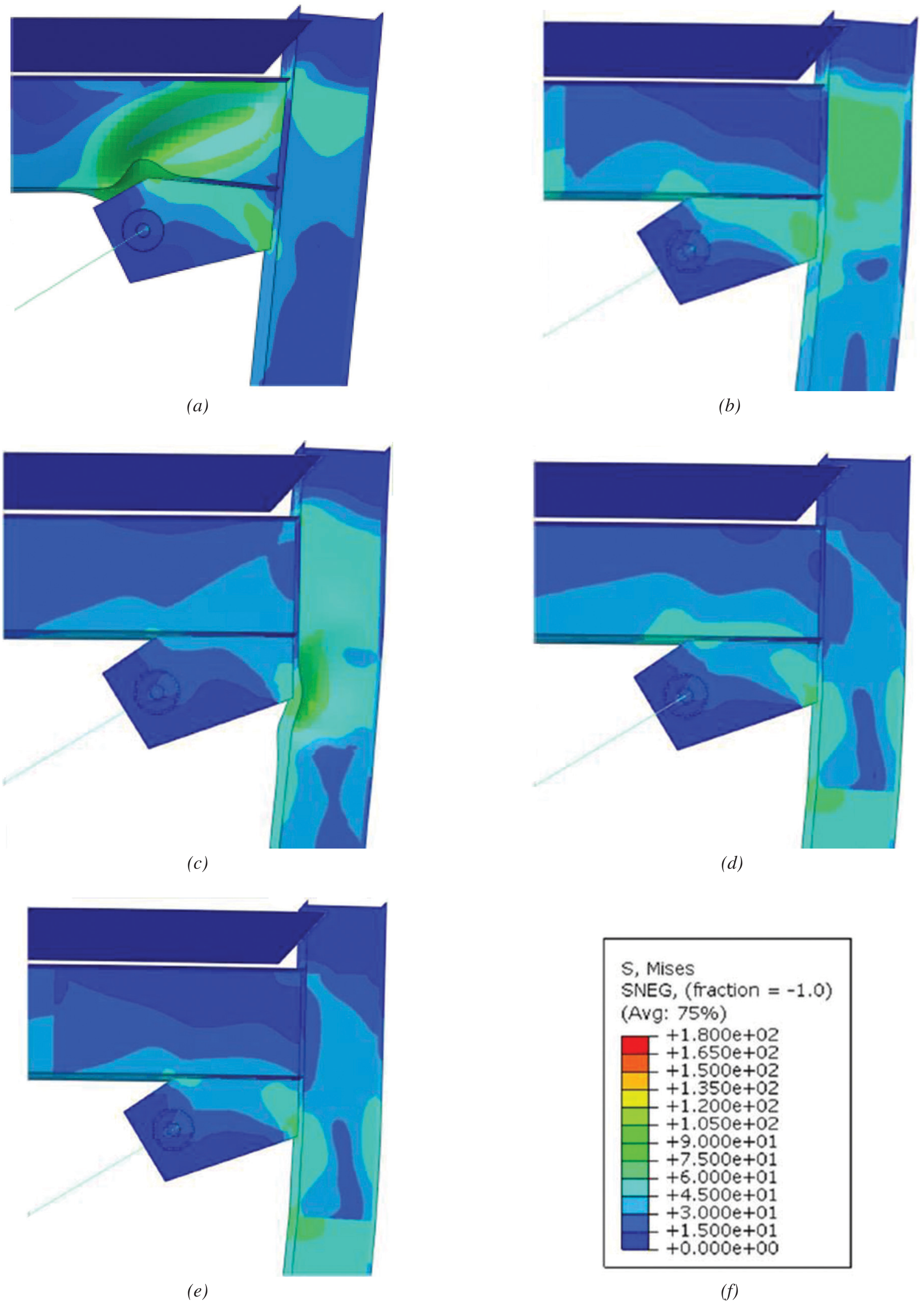

Fig. 11. Simulation results stress contours and deformed shape at 3.5% story drift (typical for deformed shapes): (a) reference model; (b) reference with 75% beam web stiffener; (c) small column model; (d) small column model with 75% column web stiffener; (e) small column model with 75% beam and column stiffeners; (f) contour legend.

Table 2. Parametric Study Response Values						
Model	Peak Base Shear, kips (kN)	Peak Moment,* kip-ft (kN-m)	Maximum PEEQ at Connection Interface (see Figure 9)			
			Beam	Column	Gusset Plate at Beam	Gusset Plate at Column
Reference	347.2 (1545)	611.8 (830)	0.286	0.106	0	0.143
Reference with 1-in. gusset plate	346.7 (1543)	612.5 (831)	0.318	0.166	0	0.055
Reference with 0.75-in. gusset plate	345.2 (1536)	578.6 (785)	0.256	0.046	0.023	0.565
Reference with 0.625-in. gusset plate	343.8 (1530)	570.5 (774)	0.233	0.03	0.047	0.689
Reference with 0.5-in. gusset plate	344.9 (1535)	542.5 (736)	0.196	0.017	0.097	0.818
Reference with 0.75-in. gusset plate and edge stiffener	344.9 (1535)	609.6 (827)	0.277	0.089	0.027	0.12
Reference with 0.5-in. gusset plate and edge stiffener	345.8 (1539)	580.1 (787)	0.208	0.03	0.112	0.354
Reference with 75% beam web stiffener	369.7 (1645)	612.5 (831)	0.087	0.114	0	0.157
Reference with 50% beam web stiffener	364.7 (1623)	614 (833)	0.175	0.11	0	0.148
Smaller column	303.4 (1350)	263.1 (357)	0.04	0.297	0	0
Smaller column with column web stiffener	312.8 (1392)	361.2 (490)	0.082	0.08	0	0.031
Smaller column with beam and column web stiffener	320 (1424)	375.9 (510)	0.026	0.08	0	0.09

* Moment in column B-1 at gusset plate edge at top of second story.

Reducing Gusset Plate Thickness

Because the relative thickness of the gusset plate to the beam and column web affects the frame damage, it is logical to think that slightly thinner gusset plates may be beneficial. The reference frame had a 1-in. (25.4-mm) gusset plate thickness, but a number of factors, including pin bearing stress, were considered in the selection of that thickness, so thinner plates may be possible. Four modifications to the reference frame were made with 0.5-, 0.625-, 0.75- and 1.25-in. (12.7-, 15.9-, 19.1- and 38.1-mm) gusset plate thickness. The 0.75- and 1.25-in. (19.1- and 38.1-mm) gusset plate satisfied all AISC *Steel Construction Manual* (2005) design limit states. The 0.5- and 0.625-in. (12.7- and 15.9-mm)-thick gusset plates did not satisfy the standard buckling expression but were included in the analysis for completeness and to assess the effectiveness of this design expression. Thinner gusset plates clearly reduced the damage and stress levels in the beam and column webs. Table 2 shows that the maximum PEEQ demand in the beam was 0.196 and 0.286 with the 0. and 1.0-in. (12 and 25-mm)-thick gusset plates, respectively. Larger reductions were noted in the column, where the maximum PEEQ was 0.017 and 0.106 with the 0.5- and 1.0-in. (12.7- and 25-mm)-thick gusset plates, respectively. These reductions in PEEQ reflect reduced strain demand and inelastic damage to the beam and the column, but there was a corresponding increase in damage to the thinner gusset plates. Buckling of the gusset plate occurred in the analysis of models with 0.5-, 0.625- and 0.75-in. (12.7-, 15.9- and 19.1-mm)-thick gusset plates. These instabilities occurred at story drifts less than 1% for the 0.5- and 0.625-in. (12.7- and 15.9-mm)-thick gusset plates and at approximately 2.5% for the 0.75-in. (19.1-mm)-thick gusset plate.

Edge stiffeners were added to thinner gusset plates along the long edge to prevent extreme deformation of the gusset, and these stiffeners reduced the damage to the gusset and correspondingly increased the damage to the beam and column so that it approximated the damage of the thicker gusset plates. This can be seen by comparison of PEEQ values in Table 2. With this evaluation, it is clear that thinner gusset plates are unlikely to be effective in reducing unwanted damage in BRBs because BRBs have large strain hardening and increasing brace forces compared to buckling brace frames.

Continuity Plates

A model with column continuity plates added at the second floor of the W12×72 column was analyzed to assess the impact on the column flange demands at the beam bottom flange. As previously discussed, the column flange was damaged at this location in a similar manner to the damage observed in moment frame columns in the 1994 Northridge earthquake (see Figure 3d). Figure 12 shows the plastic strain demand in the column flange in the elements on either side of the beam bottom flange for the models with and without the continuity plates. The continuity plate thickness was equal to one-half the beam flange thickness. The maximum strain demand occurs in the center of the column at the web location, and the demands in the column without the continuity plates are three times the demands in the column with the continuity plates, indicating a much higher likelihood of flange tearing when continuity plates are not provided.

Beam Moment Releases

Beam moment releases such as illustrated in Figure 2 and employed by Fahnestock and colleagues in a prior test program (2007) were also evaluated in a separate model. This

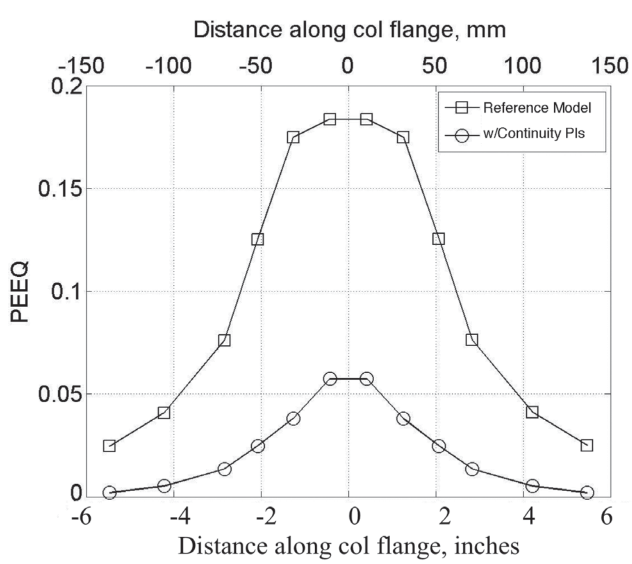

Fig. 12. Strain demand in column A-1 flange at second-floor bottom beam flange.

detail dramatically reduces the demands on both the beam and columns. It effectively eliminates the need for beam and column web stiffeners and reduces the demands on the gusset plates. However, there are some consequences of this choice. In particular, a significant rotation must be permitted in the floor beam at the edge of the gusset plate connection. Allowances in the design of the floor slab may be required to permit this rotation. More research needs to be performed on this type of connection to assess the effect of the slab before recommendations can be made regarding the use of this.

Welds Joining Gusset to Beam and Column

Weld fracture was noted in the test frame, and one model explicitly investigated the weld cracking. This model was basically the reference model, but it explicitly modeled the geometry of the fillet welds joining the gusset to the beam and column. This was accomplished by using a weld-specific constitutive model and shell elements modeling the weld geometry at the interface. The thickness assigned to the shell elements was total throat thickness of the fillet welds (⅜-in. fillets were used on both sides of the gusset plate).

The constitutive model was calibrated to match the force-normalized deformation (p) response given by Equation 1 (AISC, 2005).

$$P = 0.60F_{EXX}(1.0 + 0.5\sin^{1.5}\theta)\,[p(1.9 - 0.9p)]^{0.3} \qquad (1)$$

where P is the nominal strength of the weld segment at a deformation Δ, F_{EXX} is the weld electrode strength (70 ksi), θ is the load angle measured relative to the weld longitudinal axis and p is the ratio of element deformation Δ to its deformation at maximum stress, Δ_{max}, given by Equation 2. A load angle, θ, of 50 degrees was used because the simulations showed that the stress perpendicular to the weld was a larger component than shear. This angle results in a weld strength increase of 35% relative to a longitudinally loaded weld. The strength increase for a weld that is loaded at 90 degrees is 50%.

$$\Delta_{max} = 1.087w(\theta + 6)^{-0.65} \le 0.17w \qquad (2)$$

where w is the weld size.

In the test frame, initial tearing was observed in the gusset plate welds at a roof story-drift ratio of approximately 2.3%. The PEEQ, PE and elongation of the shell element modeling the weld were sampled in the elements at the edge of the gusset plates at this drift level, and they are listed in Table 3. Also listed are the mean values for each index and the standard deviation and the coefficient of variation (COV). The PE and PEEQ are commonly used as indicators of crack initiation and fracture, and Table 3 shows that these parameters are extremely large when the fillet welds designed by the uniform force method are considered. PEEQ

Table 3. Weld Tearing Analysis Results					
	With Weld Model			Without Weld Model	
Gusset Plate	PEEQ	PE	Elongation, in. (mm)	PEEQ	PE
2nd floor column A-1	3.6	0.23	0.0041 (0.105)	0.125	0.011
3rd floor column B-1	3.04	0.17	0.0025 (0.064)	0.149	0.0131
2nd floor column B-1	2.68	0.134	0.0019 (0.048)	0.071	0.005
Mean	3.11	0.178	0.0028 (0.072)	0.115	0.001
Standard deviation	0.463	0.049	0.0011 (0.029)	0.04	0.005
COV (%)	14.9	27.4	40.7	34.8	46.4

had the smaller COV and was used as a better indicator of weld cracking in the test frame. Cracking was observed at an average PEEQ of 3.11. Figure 13 shows the variation of the PEEQ at the three different gusset plates as a function of story drift. PEEQ is increasing rapidly at larger drift levels

A second simulation was performed with welds sized to develop the plastic tensile capacity of the gusset plate (⅞-in. fillet welds). Figure 13 also shows the PEEQ values for this model. PEEQ is dramatically smaller with the increased weld size, and crack initiation in the welds would not be expected even until deformations have increased beyond 3.25% drift. This analysis shows that the likelihood of weld tearing is significantly reduced or eliminated when the welds are designed for the strength of the plate.

DESIGN AND DETAILING RECOMMENDATIONS

Based on the experimental work and simulations described earlier, the following recommendations are made for the corner connection region of BRBF systems.

Beam

1. Beam web reinforcement should be placed at the corner gusset plate locations and extend at least to the larger of $0.75d_b$ and 12 in. (300 mm) beyond the gusset plate edge, as shown in Figure 14. This reinforcement should be placed as close to the column face as possible and will be limited by the beam web connection plates or angles. The web reinforcement should increase the total web

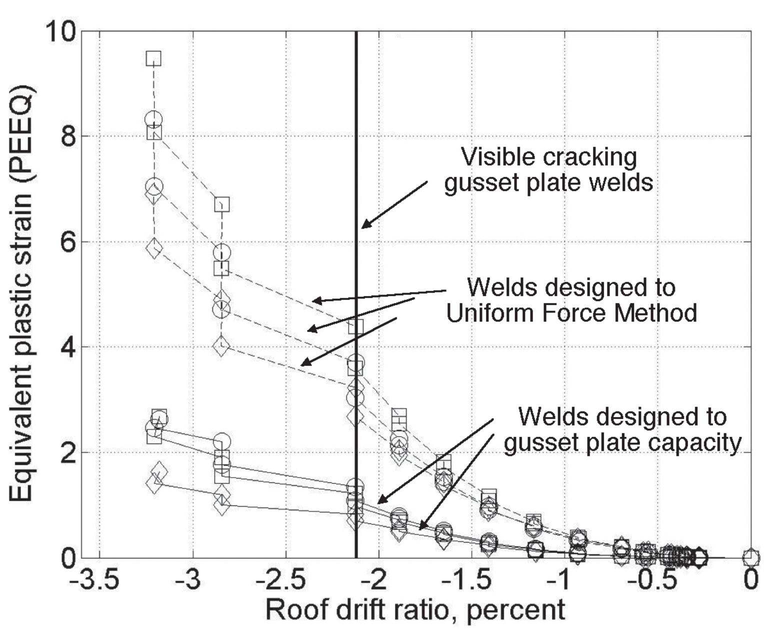

Fig. 13. Plastic strain demands at gusset plate edge.

thickness to 75% of the gusset plate thickness. This ratio may be reduced given further experimental verification.

2. Backing bars should be removed at the beam bottom flange CJP connection to the column, as they are required in special moment frames per the *Seismic Provisions*, unless there is a gusset plate connection to the column and bottom flange of the beam.

Column

3. Column web reinforcement should be installed in the panel zone and within the gusset region and extend at least to the larger of $0.75d_c$ and beyond the gusset plate edge as shown in Figure 14. The web reinforcement should increase the total web thickness to 75% of the gusset plate thickness.

4. Continuity plates should be provided in the column at the beam flanges according to the *Seismic Provisions* when the beam flanges are connected to the column and expected to behave as a partially or fully restrained connection (Figure 14).

Gusset Plate

5. The current LRFD gusset plate design limit states should be used, except all welds connecting the gusset plate to the beams and columns should be CJP welds or fillet welds with a strength equal to the yield capacity of the gusset plate. The expected yield strength of the plate, R_yF_y, should be used in this calculation.

SUMMARY AND CONCLUSIONS

BRBFs are a commonly used seismic resisting system. However, most studies have focused on the BRB and neglected its interaction with the adjacent components. Recent tests indicate that unwanted damage modes are sustained by BRBFs, including local buckling of the beams and tearing of the interface weld. To improve the response and mitigate these mechanisms, an analytical study was undertaken. The study used an experimental study of a two-story frame as its basis. Using high-resolution modeling techniques, a validated model was developed. This model was then used to perform a parametric study. The primary objectives of the study were to quantify the effects of various parameters on the demands and behaviors of the joint region and develop verified design and detailing recommendations to improve the performance of these systems.

The study resulted in the following conclusions:

1. Reducing the gusset plate thickness reduced the demands in the beam and column at the gusset interfaces. However, buckling of the gusset plate limits how thin these can be. Therefore, this is not an effective way of reducing component demands in the connection region of BRBFs. This is different than recommendations for SCBFs because buckling braces are a softening system after brace buckling, while BRBFs continue to sustain large increases in brace force after yielding of the BRB.

2. Analyses shows that designing the weld for the strength of the plate significantly reduces the local strain demand in the connection and is expected to reduce crack initiation and prevent weld tearing and fracture until much larger story drifts. Therefore, weld connecting the

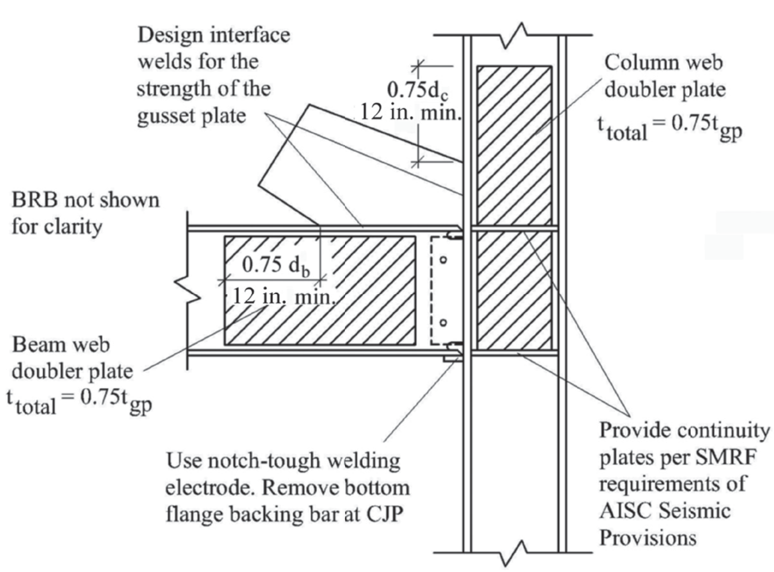

Fig. 14. Recommended detailing at corner connection region of BRBF.

gusset plate to the beam and column should be sized to meet the strength of the gusset plate to mitigate weld tearing.

3. A smaller column reduced the demands in the beam, including local web and flange deformation at all drift levels. However, the demand and deformation in the column was increased. Adding column web reinforcement within the gusset region mitigated these demands and deformations, and while this caused a slight increase in beam demands, the resulting beam demands were still considerably less than those seen in the reference model and had negligible impact on the behavior and performance of the beam. In lieu of adding doubler plates, it may be more economical to increase the column or beam shape to a size that has an appropriate web thickness but may be overdesigned for flexure and axial load.

4. The demands and local deformation in the beams and columns within the connection region were shown to be inversely proportional to the ratio of the beam web thickness to the thickness of the gusset plate. In other words, for a given beam or column size, a thick gusset plate will increase the demands on these elements relative to a thinner gusset plate. These demands are also dependent on other factors, such as the relative beam and column size and the mechanism used to accomplish the target thickness ratio (e.g., thin gusset plate versus adding a web reinforcement). Given that there is a limit on how thin a gusset plate can be due to potential buckling, adding beam web reinforcement is a more appropriate solution to mitigate damage. Adding beam web reinforcement such that the web to gusset plate thickness ratio was 0.75 is recommended.

ACKNOWLEDGMENTS

The authors gratefully acknowledge the support of the National Science Foundation's Network for Earthquake Engineering Simulation (Grant No. CMS-619161) and the American Institute of Steel Construction. The opinions and findings expressed here are those of the authors alone and do not necessarily reflect the views of the sponsoring agencies.

REFERENCES

ABAQUS (2010), *ABAQUS version 6.10 documentation*, Simulia.

AISC (2005), *Steel Construction Manual,* 13th ed., American Institute of Steel Construction, Chicago, IL.

AISC (2010), *Seismic Provisions for Structural Steel Buildings,* ANSI/AISC 341-10, American Institute of Steel Construction, Chicago, IL.

Black, C., Makris, N. and Aiken, I. (2004), "Component Testing, Seismic Evaluation and Characterization of Buckling-Restrained Braces," *Journal of Structural Engineering*, Vol. 130, No. 6, pp. 880–894.

Chao, S.H., Khandelwal, K. and El-Tawil, S. (2006), "Ductile Web Fracture Initiation in Steel Shear Links," *Journal of Structural Engineering*, Vol. 132, No. 8, pp. 1192–1200.

Chen, C., Lai. J. and Mahin, S. (2008), "Seismic Performance Assessment of Concentrically Braced Steel Frame Buildings," *Proceedings of the 14th World Conference on Earthquake Engineering*, Beijing, China.

Christopolus, A.S. (2005), "Improved Seismic Performance of Buckling Restrained Braced Frames," M.S. Thesis, University of Washington, Seattle, WA.

El-Tawil, S., Mikesell, T. and Kunnath, S.K. (2000), "Effect of Local Details and Yield Ratio on Behavior of FR Steel Connections," *Journal of Structural Engineering*, Vol. 126, No. 1, pp. 79–87.

Fahnestock, L.A., Ricles, J.M. and Sause, R. (2007), "Experimental Evaluation of a Large-Scale Buckling-Restrained Braced Frame," *Journal of Structural Engineering*, Vol. 133, No. 9, pp. 1205–1214.

Hancock, J.W. and Mackenzie, A.C. (1976), "On the Mechanics of Ductile Failure in High-Strength Steel Subjected to Multi-Axial Stress States," *Journal of Mechanical and Physical Solids*, Vol. 24, pp. 147–169.

Kanvinde, A. and Deierlein, G. (2006), "Void Growth Model and Stress Modified Critical Strain Model to Predict Ductile Fracture in Structural Steels," *Journal of Structural Engineering*, Vol. 132, No. 12, pp. 1907–1918.

Meritt, S., Uang, C. and Benzoni, G. (2003), "Subassemblage Testing of Star Seismic Buckling-Restrained Braces," Report No. TR-2003/04, University of California, San Diego, La Jolla, CA.

Palmer, K.D. (2012), "Seismic Behavior, Performance and Design of Steel Concentrically Braced Frame Systems," Ph.D. Dissertation, University of Washington, Seattle, WA.

Palmer, K.D., Christopulos, A.S., Lehman, D.E. and Roeder, C.W. (2014), "Experimental Evaluation of Cyclically Loaded, Large-Scale, Planar and 3-D Buckling-Restrained Braced Frames," submitted for publication review, *Journal of Constructional Steel Research,* Elsevier.

Romero, P., Reaveley, L., Miller, P. and Okahashi, T. (2007), "Full Scale Testing of WC Series Buckling-Restrained Braces," Final Report to Star Seismic, University of Utah, Salt Lake City, UT.

Uriz, P. (2005), "Towards Earthquake Resistant Design of Concentrically Braced Steel Structures," Ph.D. Dissertation, University of California, Berkeley.

Wigle, V.R. and Fahnestock, L.A. (2010), "Buckling-Restrained Braced Frame Connection Performance," *Journal of Constructional Steel Research*, Vol. 66, pp. 65–74.

Yoo, J. (2006), "Analytical Investigation on the Seismic Performance of Special Concentrically Braced Frames," Ph.D. Dissertation, University of Washington, Seattle, WA.